Effects of High Sound Pressure Levels in a Model of the Normal and Impaired Auditory Periphery

M. S. Arefeen Zilany (zilany@grads.ece.mcmaster.ca) and **Ian C. Bruce**
Department of Electrical and Computer Engineering, McMaster University, Hamilton, Ontario, Canada

1. Introduction

Computational models have been developed by Carney and colleagues to simulate the responses of auditory nerve (AN) fibers in cat (Carney, JASA 1993; Zhang et al., JASA 2001; Tan and Carney, JASA 2003). The most recent version adds a level-independent instantaneous frequency glide in the basilar membrane (BM) filter, as observed in BM and AN data. This model produces realistic responses to simple acoustic stimuli but has not applied to the study of AN responses to speech. The Zhang et al. (2001) version of the model has been modified by Bruce and colleagues (JASA 2003) to study the effects of outer and inner hair cell impairment on the AN's representation of speech stimuli. However, the Bruce et al. model did not address the instantaneous frequency glides in the impulse response of AN fibers, which may explain the shifts in best frequency (BF) following impairment of outer hair cells or at high intensities in the normal cochlea. All of the previous model of this type did not address component 1/ component 2 (C1/C2) transition, one of the most important physiological phenomenon observed near 90-100 dB SPL in the rate- and phase- level functions of AN fibers. In this paper, an improved model has been developed to explain these high level effects on the neural representation of speech in normal and impaired ears. The motivation for the development of this model is to provide a more accurate description of the responses of AN fibers to speech sounds at high sound pressure levels that might be useful in testing the effects of potential hearing-aid speech processing schemes.

2. The Model

The model of Bruce and colleagues is an extended version of the previous model developed by Zhang et al. (2001), which included the compressive changes in gain and bandwidth as a function of stimulus level, the associated changes in the phase of the phase locked responses and two-tone suppression. In the Bruce et al. model, the wide-band feedforward control path was modified and a middle ear filter was added, both of which helped improve the model's response to wide-band stimuli such as speech signals. However, replacing the BM filter of the Bruce et al. model by a chirp filter that produces frequency glides in the impulse response of AN fibers enhances the ability of the model to predict AN responses to speech stimuli. Furthermore, a component 2 filter is introduced into the model parallel to the BM filter whose behaviour is similar to the BM filter with the outer hair cell completely impaired. Inversion of the C2 filter output by a linear transduction function (cf. the nonlinear transduction function after the C1 filter) produces a 180° phase shift. The interactions of the parallel BM filter paths explain the C1/C2 transition that is characterized by an abrupt shift of 180° in the phase of the response and sometimes also by a dip in the average rate at the same levels. In addition, the parameters of the Boltzmann function in the control path is modified somewhat to explain some of the reported speech data more accurately.

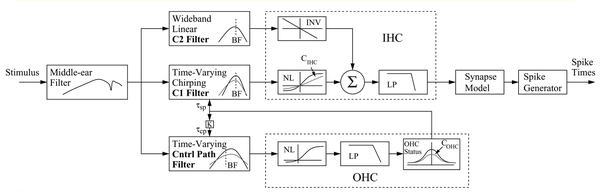

Fig. 1. Schematic diagram of the proposed auditory-periphery model. Abbreviation: outer hair cell (OHC), inner hair cell (IHC), low-pass filter (LP), static nonlinearity (NL), best frequency (BF), component 1 filter (C1), component 2 filter (C2), inverting linear function (INV).

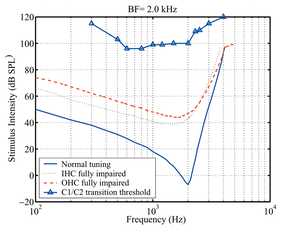

Fig. 2. Model tuning curves for BF = 2.0 kHz. Solid (blue) is for normal tuning curve with no impairment, C_{OHC} = 1.00, C_{IHC} = 1.00; dotted (green) is for impaired tuning with complete impairment in inner hair cell, C_{IHC}= 0.00; dashed (red) is model tuning with complete outer hair cell impairment C_{OHC} = 0.00; upper triangle shows the C1/C2 transition threshold tuning curve.

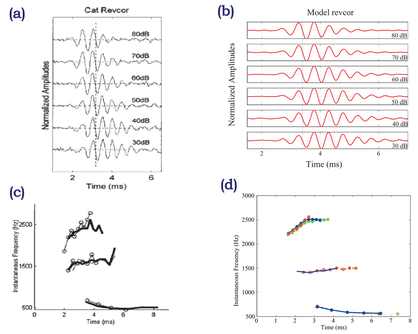

Fig. 3. Revcor functions and instantaneous frequency profiles (a)Measured revcor functions for AN fiber with BF = 2060 Hz at six levels: 30 to 80 dB SPL (unit 86100-25 from Carney and Yin,1988) (b) Model revcor functions for a fiber with matching BF. All revcor functions are normalized to their peak amplitude. (c) Measured AN instantaneous frequency glides calculated based on zero-crossings from revcor functions with 40, 60 and 80 dB for BFs 550, 1600 and 2500 Hz. (d) Model AN instantaneous frequency profiles for fibers with BFs matching the measured fibers. It shows that instantaneous-frequency glides are almost level- independent.

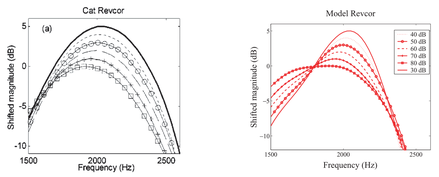

Fig. 4. Measured and model reverse-correlation filters. The magnitudes of the revcor filters were computed for wideband noise presented at stimulus levels from 30 to 80 dB SPL. Each revcor filter is normalized by its peak value; for clarity, a 1-dB shift is introduced between filters computed at different noise levels. The measured responses are from unit 86100-25 from Carney and Yin (1988).

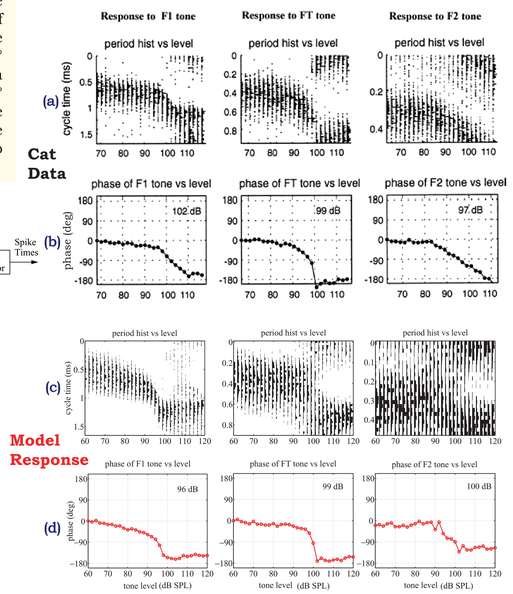

Fig. 5. The tone responses of a representative fiber. The fiber's BF is 2.03 kHz. The tone frequencies used are F1=0.6 kHz, FT= 1.07 kHz, and F2= 2.03 kHz. (a) Dot plots redrawn from Fig.1 of Wong et al. (1988) showing period histogram along the ordinate across the range of sound levels. Displays are constructed by placing a dot at the stimulus phase of each action potential in the response, at each sound level. (b) Average phase of responses plotted vs sound level, redrawn from Fig.1 of Wong et al. (1988). (c) Dot plots for the model response. (d) Average phase for the model response.

3. Results

The basic response properties of the model are quite satisfactory, as shown in the figures. Also, the model C1/C2 transitions for three different tones shown in the fig. 5 give a fairly good match to the results reported by Wong et al. (1998).

Predictions shown in fig. 6 have been obtained for model fibers with BFs roughly covering the range of BFs in the Wong et al. (1998) data. Consistent with the physiological data, the new model predictions for normal OHC and IHC function exhibit synchrony capture by F2 at moderate levels. Also seen in the model predictions is the transition in synchrony from F2 to F1 at higher intensities and the stimulus intensity at which the switch occurs is decreasing with incresing BF. The new model better predicts this switch in synchrony capture than the Bruce et al. model.

In fig. 7, the model predictions for both normal and impaired fibers are predominantly within the range of values seen in the physiological data. Normal fibers synchronize almost exclusively to the formant frequency closest to their BFs. The small peak in F1 PR of the model predictions at 1 kHz is due to the harmonic distortion in the nonlinear BM filter. With impaired OHC and IHC function, model predictions of PRs fall within the range of single-fiber values for F1, F2 and F3 quite reasonably. An upward shift in the peaks of F1 and F2 synchrony is observed in the model predictions, consistent with the physiological data.

Fig. 6. Normal power ratio (PR) data at high sound levels for four normal fibers with BFs as labeled. The solid and dashed lines, respectively, show the fraction of total power in the fiber's response that is synchronized to F1 and F2 combined (F1 & F2) or to F2 alone. Total power is the sum of the squares of the synchronized rates over the first 20 harmonics of the stimulus. F1 & F2 related power is the sum of the squares of the synchronized rates at the harmonics related to F1 and F2, which include the 5th, 7th, 10th, 12th,15th, 17th and 20th harmonics. The F2 PR is the fraction of the total power that is phase-locked to the second formant (17th harmonic). The F1 & F2-related PR is the fraction of the total power contained in the f1 & F2-related harmonics. The lower and upper bounds of the shaded regions represents, respectively, the sound levels at which a loss of synchrony capture by F2 occurs and the component 2 threshold for F1. Left column: Redrawn from Fig.4 of Wong et al. (1988). Middle column: Results from Bruce et al. (2003). Right column: Results from the proposed model.

[This work was supported by NSERC Discovery Grant 261736 and the Barber-Gennum Chair Endowment.]

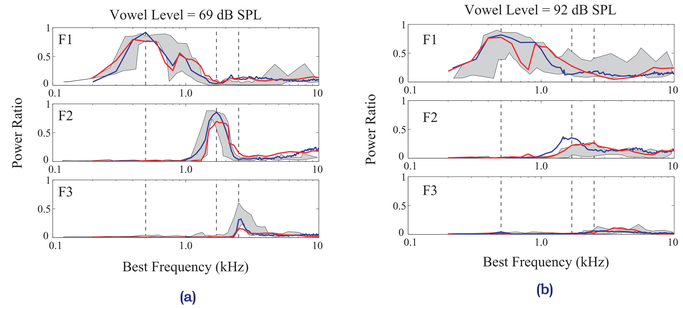

Fig. 7. (a) Model predictions of normal power ratios for F1, F2 and F3 as a function of normal BF for stimulus intensities of 69 dB SPL. (b) Model predictions of impaired power ratios for the 3 formants as a function of impaired BF for stimulus intensities of 92 dB SPL. Thick lines show model predictions (**Blue: Bruce et al. Model** 2003, **Red: Proposed Model**) and gray hatched area indicate the range of values observed in normal (a) and impaired (b) physiological data of Miller et al. (1997). Vertical dashed lines show the formant frequencies. Predictions are shown for model Q_{10} values that are 50^{th} percentile of the Q_{10} values for the normal (a) and impaired (b) physiological data. PRs here include the phase-locked response to the first, second and third harmonics of the formant frequency, as long as the frequency of the harmonic is less than or equal to 5 kHz.

4. Discussions and Conclusions

This poster describes a computational model that is accurate enough to be useful in testing the effects of potential hearing aid processing schemes on the neural representation of speech. The added feature of level-independent frequency glides in the impulse response of AN fibers into the Bruce et al. model gives more realistic AN responses for the vowel stimuli. The realization of BF shift in the impaired cochlea or at high intensities in the normal cochlea in this model helps to describe the loss of synchrony from the second formant to the first at high intensities or in the impaired cochlea. The parameters of the Boltzmann function in the control path shows a significant effect on the behaviour of compression which is partly responsible for the loss of synchrony from F2 to F1 at high intensities.

To describe one of the most important high-level effects, the C1/C2 transition, a C2 filter is implemented in parallel with the primary BM filter (C1 filter), and two different IHC transduction functions are utilized. Note that the C2 filter has the same frequency response as the C1 filter at high levels or with full OHC impairment—this is not a "tail filter" as utilized in some other cochlear models. The nonlinear transduction function following the C1 filter exhibits saturation and is sensitive to impairment, whereas the inverting transduction function following the C2 filter does not saturate and is insensitive to impairment. This implementation is in agreement with Kiang's (1990) two-factor cancellation hypothesis that C1 is sensitive and operating at low levels and C2 is insensitive and shifted in phase by 180° relative to C1. The growth of C2 is such that it is significantly smaller than C1 at low levels and becomes significantly larger than C1 at high levels. The phase transition and rate dip reflects the cancellation of the two components where they are approximately equal in amplitude.

These additions to the previous model improve its accuracy and utility as a means of developing and testing potential hearing-aid speech processing schemes for sensorineural hearing loss.

References

[1] Bruce IC, Sachs MB, Young ED. An auditory-periphery model of the effects of acoustic trauma on auditory nerve responses. J. Acoust. Soc. Am. 113: 396–388, 2003.

[2] Tan Q, Carney LH. A phenomenological model for the responses of auditory-nerve fibers. II. Nonlinear tuning with a frequency glide. J. Acoust. Soc. Am. 114: 2007-2020, 2003.

[3] Carney LH. A model for the responses of low-frequency auditory-nerve fibers in cat. J. Acoust. Soc. Am. 93: 401-417, 1993.

[4] Zhang X, Heinz MG, Bruce IC, Carney LH. A phenomenological model for the responses of auditory-nerve fibers: I. Nonlinear tuning with compression and suppression. J. Acoust. Soc. Am. 109: 648–670, 2001.

[5] Carney LH, McDuffy MJ, Shekhter I. Frequency glides in the impulse responses of auditory-nerve fibers. J. Acoust. Soc. Am. 105: 2384-2391, 1999.

[6] Wong JC, Miller RL, Calhoun BM, Sachs MB, Young ED. Effects of high sound levels on responses to the vowel /ɛ/ in cat auditory nerve. Hearing Research. 123: 61-77, 1998.

[7] Miller RL, Schilling JR, Franck KR, Young ED. Effects of acoustic trauma on the representation of the vowel /ɛ/ in cat auditory-nerve fibers. J. Acoust. Soc. Am. 101(6):3602–3616, 1997.

[8] Kiang NYS. Curious oddments of auditory-nerve studies. Hearing Research 49: 1-16, 1990.

[9] Liberman MC, Kiang NYS. Single-neuron labeling and chronic cochlear pathology. IV. Stereocilia damage and alterations in the rate- and phase- level functions. Hearing Research 16: 75-90, 1984.